

Machine Learning Methods in Geoscience

Gerard T. Schuster with labs by Yuqing Chen, Yongxiang Shi, Shihang Feng,
Zhaolun Liu, Zongcai Feng, Yunsong Huang, Yan Yang and Tushar Gautam

March 14, 2022

Contents

Preface	xv
Notation Convention	xxiii
Abbreviations	xxvii
1 Introduction to ML in Geosciences	1
1.1 Introduction	1
1.2 Three Classes of Machine Learning	5
1.2.1 Supervised Learning	5
1.2.2 Unsupervised Learning	7
1.2.3 Reinforcement Learning	7
1.3 Summary	9
I Mathematical Background	13
2 Data Prediction by Least Squares Inversion	15
2.1 Least Squares Inversion	15
2.1.1 Overdetermined, Inconsistent, and Ill-conditioned Equations	16
2.1.2 Least Squares Solution	16
2.1.3 Regularized Least Squares Solution	21
2.1.4 Geometrical Interpretation of Gradient $\nabla\epsilon$	26
2.1.5 Preconditioning	28
2.1.6 Overfitting Data	29
2.1.7 Inclusion of Bias Factor	34
2.2 Steepest Descent Optimization	34
2.3 Non-Linear Optimization	36
2.3.1 MATLAB Examples of Newton's Method	37
2.4 Summary	41
2.5 Exercises	42
2.6 Appendix: Exact Step Length	46

3	Specialized Gradient Descent Methods	49
3.1	Ad Hoc Gradient Descent Methods	49
3.1.1	Momentum Gradient Descent	49
3.1.2	Adagrad Gradient Descent	56
3.1.3	Adadelta Gradient Descent	58
3.1.4	Nesterov Accelerated Gradient (NAG)	59
3.1.5	Adam Gradient Descent	60
3.1.6	AdaMax Gradient Descent	63
3.1.7	Hybrid Step-length Strategy	63
3.2	Numerical Line Search	64
3.3	Conjugate Gradient	64
3.3.1	MATLAB Conjugate Gradient Code	67
3.4	Summary	70
3.5	Exercises	71
3.6	Appendix: Rosenbrock Plotting Code	73
3.7	Appendix: Step Length Plotting Codes	73
II	Supervised Learning	75
4	Introduction to Neural Networks	77
4.1	Introduction	78
4.1.1	Biological Inspiration of a Neural Network	80
4.1.2	General Neural Network	83
4.1.3	Geometrical Interpretation of a Neural Network	86
4.1.4	Generality of a Neural Network	88
4.1.5	Neural Network Workflow	91
4.1.6	Recursive Feed-forward Formula	91
4.1.7	Recursive Back-propagation Formula	93
4.2	Activation Functions	95
4.3	Examples of Neural Networks	98
4.3.1	Single-Layer Neural Network	99
4.3.2	Two-layer Neural Network	100
4.3.3	Neural Network MATLAB Code	103
4.3.4	NN with a Cross-Entropy Objective Function	104
4.4	Types of Classification	111
4.4.1	Multilabel Classification	111
4.4.2	Multiclass Classification	111
4.5	Best Practices	114
4.6	Summary	121
4.7	Exercises	124
4.8	Computational Labs	132
4.9	Appendix: Neural Network Workflow	132
4.10	Appendix: MATLAB Code for Validation	135

5	Processing Data with FCNN	137
5.1	FCNN Filtering of Migration Images in $\mathbf{z} = (x, z)$	137
5.2	Filtering Angle-Domain Images	141
5.2.1	Angle Domain Transform	141
5.2.2	Filtering Marine Data	143
5.3	NN Filtering of Surface Waves	144
5.4	MATLAB Codes	147
5.5	Summary	149
5.6	Exercises	150
5.7	Computational Labs	150
5.8	Appendix: skeletonized Characteristics in an Image	150
5.9	Appendix: MATLAB Code for Logistic Regression	151
6	Multilayer FCNN	155
6.1	Introduction	155
6.2	Feed-forward Operation	155
6.3	Back-propagation Operation	156
6.3.1	Formula for $\partial\epsilon/\partial w_{jk}^{[N]}$	157
6.3.2	Formula for $\partial\epsilon/\partial w_{ij}^{[N-1]}$	157
6.3.3	Formula for $\partial\epsilon/\partial w_{ij}^{[N-2]}$	158
6.4	MATLAB Code	160
6.5	Summary	162
6.6	Exercises	163
6.7	Computational Labs	163
6.8	Appendix: Vectorized Steepest Descent Formula	163
7	Support Vector Machines	165
7.1	Introduction	165
7.2	SVM Theory	166
7.2.1	SVM Applications	167
7.3	Linear SVM	169
7.4	Nonlinear SVM	172
7.5	Primal and Dual Solutions	174
7.6	Kernel Methods	177
7.7	Numerical Examples	181
7.7.1	MATLAB Codes	182
7.8	Multiclass SVM	183
7.9	Hinge-Loss and Soft-Margin SVM	183
7.10	SVM Lab with CoLab	187
7.11	SVM Regression	192
7.12	Practical Issues for Implementing SVM	192
7.12.1	Scaling	193
7.12.2	Data Augmentation	193
7.12.3	Computational Cost	193
7.12.4	Procedures for Users	195

7.13	Summary	195
7.14	Exercises	197
7.15	Computational Labs	197
7.16	Appendix: Defining the Dual Problem with a Lagrangian	197
7.16.1	Simple Example of a Dual Solution	200
7.16.2	Concavity and Maximization of the Reduced Lagrangian	202
7.17	Appendix: Karush-Kuhn-Tucker Conditions	203
III	Convolutional Neural Networks	205
8	Convolution and Correlation	207
8.1	Convolution	207
8.1.1	Time or Shift Invariance	208
8.1.2	1D Convolution	210
8.1.3	2D Convolution	212
8.1.4	3D Convolution	213
8.2	Correlation and Matched Filters	213
8.2.1	Multilayer and Multifilter Convolution	217
8.3	Summary	220
8.4	Exercises	220
9	Convolutional Neural Networks	223
9.1	Introduction	223
9.1.1	Brief History of CNN	224
9.2	Building Blocks of CNN	227
9.2.1	CNN Forward Modeling	228
9.2.2	Model Update by Back-propagation	233
9.2.3	Keras Code	235
9.2.4	Visualizing the Filters as Correlation Functions	238
9.2.5	Visualizing the Images Associated with Feature Maps	240
9.2.6	Regularization	242
9.2.7	Mini-Batch, Step Length, Training and Data Augmentation	246
9.3	Architectures of CNN	247
9.3.1	AlexNet	247
9.3.2	VGGNet	248
9.3.3	ResNet	248
9.4	Deep Learning Software	250
9.5	Seismic Fault Detection by CNN	251
9.6	Summary	253
9.7	Exercises	254
10	Object Identification by CNN	257
10.1	Introduction	257
10.2	Image Classification	258
10.2.1	Global Picture-size Classification	258

10.2.2	Localize and Classify a Single Object	258
10.2.3	Judging the Accuracy of the Predicted BB: IOU	262
10.2.4	Localize and Classify Multiple Objects	262
10.2.5	Pixel-size Classification: Semantic Segmentation	270
10.3	Labeling Tools	270
10.4	Salt Body Detection by AlexNet	272
10.4.1	AlexNet CNN Architecture	273
10.4.2	Numerical Results	273
10.4.3	Monoparameter CNN	273
10.4.4	Multiparameter CNN	274
10.5	Detection of Rock Cracks by AlexNet	274
10.5.1	Unbalanced Crack Data	276
10.5.2	Numerical Results	276
10.6	Detection of Basalt in GPR Images	278
10.6.1	Numerical Results	281
10.7	Fault Detection and Deconvolution	283
10.8	Salt Boundary Detection by U-Net	286
10.8.1	Keras U-Net Code	290
10.8.2	Numerical Results	293
10.9	Fault Detection by U-Net	298
10.10	R-CNN Labeling of Blood Cells	298
10.11	Small Object Detection by Superpixel-based CNN	301
10.11.1	Superpixel Convolution Method	302
10.11.2	Numerical Results	303
10.12	Super-resolution Image Enhancement by CNN	307
10.13	Identification of Bird Types by CNN	308
10.13.1	Data Description and AlexNet model	309
10.13.2	Numerical Results	309
10.14	Summary	310
10.15	Exercises	310
10.16	Computational Labs	312
10.17	Appendix: Selective Search	312
10.18	Appendix: MATLAB Code for AlexNet Crack Detection	314
10.19	Appendix: Simple Linear Iterative Clustering (SLIC)	316
11	Semantic Segmentation of Cracks in Photos	323
11.1	Introduction	323
11.2	Detection and Labeling of Cracks by U-Net	323
11.2.1	Labeling Cracks	324
11.2.2	Phase I Training and Validation	325
11.2.3	Phase I Testing	327
11.2.4	Phase II Training and Validation	328
11.2.5	Phase II Testing	328
11.3	Transfer Training	332
11.4	Summary	333

11.5	Computational Labs	333
12	Recurrent Neural Networks	337
12.1	Theory of Recurrent Neural Networks	338
12.1.1	Vanilla RNN Workflow	338
12.1.2	Vanishing Gradient of VRNN	344
12.2	Gated Recurrent Unit Network	348
12.3	Training RNNs	351
12.3.1	Truncated Back-propagation	351
12.3.2	Bidirectional RNN	351
12.3.3	Deep RNN	352
12.4	RNN Applications in Geoscience	354
12.4.1	Predicting Missing Well Logs by BRNN	354
12.4.2	Predicting Well Logs from Seismic Reflection Data	354
12.5	Summary	356
12.6	Exercises	358
12.7	Computational Labs	358
12.8	Appendix: Vanishing Gradients	358
12.9	Appendix: Long Short-Term Memory Architecture	361
13	Self-attention and Transformers	367
13.1	Attention	367
13.2	Trained Attention	370
13.2.1	Single- and Multi-head Attention Architectures	374
13.3	Transformer Architecture and Training	378
13.4	Advances in Transformer Models	379
13.4.1	Transformer Models and Event Picking in Seismograms	380
13.5	Summary	383
13.6	Exercises	384
IV	Unsupervised Learning	385
14	Autoencoders	387
14.1	Theory of Autoencoders	390
14.1.1	Linear Autoencoder and PCA	393
14.2	Problems with Autoencoders	394
14.3	Regularization of Autoencoders	395
14.3.1	Dropout	397
14.3.2	Denosing Autoencoders	397
14.3.3	Contractive Autoencoders	398
14.3.4	Sparse Autoencoders	399
14.3.5	Variational Autoencoder	400
14.3.6	Adversarially Constrained Autoencoder Interpolation	404
14.4	Numerical Examples	406
14.4.1	Seismic Interpolation Example	406

14.4.2	Seismic Tomography	407
14.4.3	4D Seismic Image Monitoring and Forecasting	411
14.5	Summary	414
14.6	Exercises	415
14.7	Appendix: Autoencoder in Keras	416
14.8	Appendix: Dropout=Regularization	419
14.8.1	Least Squares Minimization with Dropout	420
14.9	Appendix: KL Regularization	421
15	Convolutional Sparse Coding	423
15.1	Introduction	423
15.2	Theory	424
15.2.1	Generalization of the Objective Function	425
15.2.2	Workflow	426
15.3	Numerical Examples	427
15.3.1	Synthetic Test	427
15.3.2	Field Data Test	428
15.4	Discussion	430
15.5	Summary	434
15.6	Computational Labs	438
15.7	Appendix: ADMM	438
16	Principal Component Analysis	441
16.1	Introduction	441
16.1.1	Historical Background of PCA	444
16.2	Theory of Principal Component Analysis	446
16.2.1	Intuitive Dinosaur Example	448
16.2.2	Simple Two-Point Example	448
16.2.3	Filtering the PCA Components	450
16.2.4	PCA Workflow	451
16.2.5	Singular Value Decomposition	453
16.3	Numerical Examples	455
16.3.1	Yellowstone Eruption Data	455
16.3.2	Biplots and Geochemical Data from a Gold Site	458
16.3.3	Nashville Limestones	458
16.3.4	PCA Applied to Hyperspectral Images	460
16.4	Kernel PCA	466
16.5	Computational Costs	467
16.6	Summary	468
16.7	Exercises	469
16.8	Computational Labs	472
16.9	Appendix: Mathematics of Kernel PCA	473
16.10	Appendix: MATLAB Kernel PCA CoLab	475

17 Clustering Algorithms	479
17.1 Introduction	479
17.2 K-means Clustering	482
17.2.1 K-means Cluster Lab with Colab	485
17.3 Agglomerative Clustering	486
17.4 Information Weighted Clustering	491
17.5 Fuzzy Clustering	492
17.5.1 Arrival Time Picking and Fuzzy Clustering	493
17.6 Elbow Method for Determining the Number of Clusters	497
17.7 Support Vector Clustering	499
17.8 DBSCAN	502
17.8.1 DBSCAN Lab with Colab	506
17.9 K-Nearest Neighbors Algorithm	507
17.10 Self-organizing Map	508
17.10.1 MATLAB SOM Examples	512
17.11 Numerical Examples	516
17.11.1 Picking Stacking Velocities by K-means Cluster Analysis	516
17.11.2 Generating Models with Sharp Impedance Contrasts	522
17.11.3 DBSCAN Applied to Earthquakes	524
17.11.4 Self-Organized Maps and Classification of Porosity in Rocks	532
17.11.5 Self-Organized Maps and Classification of Seismic Horizons	538
17.11.6 Self-Organized Maps and Fault Detection	539
17.12 Summary	539
17.13 Exercises	540
17.14 Computational Labs	541
17.15 Appendix: Derivation of the Fuzzy Clustering Weight	541
18 Generative Adversarial Networks	545
18.1 Introduction	545
18.2 Theory of GANs	547
18.2.1 GAN Objective Function and Minimax Algorithm	548
18.3 Pseudo-Code for a GAN	550
18.4 Simple Fault Example	555
18.5 GAN Examples in Geoscience	557
18.5.1 Seismic-to-Attribute Sections by a GAN	557
18.5.2 Seismic Resolution Enhancement by GANs	559
18.6 Summary	559
18.7 Exercises	562
18.8 Appendix: GAN Examples	563
V Bayesian Analysis	567
19 Sampling a Probability Distribution	569
19.1 Sampling a Probability Distribution	569

19.2	Sampling a PDF by the Inverse-Transform	572
19.3	Sampling a PDF by Acceptance-Rejection	572
19.4	Markov Chain	576
19.5	Metropolis Markov Chain Monte Carlo Sampling	578
19.5.1	Detailed Balance Equation	580
19.5.2	Metropolis Sampling Example	581
19.6	Gibbs Sampling	583
19.7	Summary	587
19.8	Exercises	588
19.9	Appendix: MATLAB Functions for Metropolis Code	588
20	Bayes' Theorem	591
20.1	Introduction	591
20.2	Intuitive Interpretation of Bayes' Theorem	594
20.2.1	Geometrical Interpretation of $P(C), P(T), \frac{P(C)}{P(T)}$	595
20.2.2	Medical Interpretation of $P(C), P(T), \frac{P(C)}{P(T)}$	596
20.2.3	Updating Predictions with New Information	598
20.3	Naive Bayes' Theorem	599
20.4	Motivation for Bayes' Theorem	599
20.5	BI and Regularized Least Squares Inversion	600
20.6	Geophysical Examples of Bayesian Inversion	602
20.6.1	Prediction of an Oil-Spill Source	602
20.6.2	VSP Traveltime Inversion	605
20.6.3	Imaging Point Sources in a Hydrofrac Experiment	613
20.6.4	Rock Types and Uncertainty from Well Log Data	617
20.6.5	Rock Types from Well Logs and Seismic Data	624
20.7	Summary	624
20.8	Exercises	628
20.9	Appendix: Bayes' Theorem Examples	630
20.9.1	Example: Rainy Weather	630
20.9.2	Example: Biking and Weather	632
20.10	Appendix: Naive Bayes' Theorem, Weather and Biking	634
20.11	Appendix: Kullback-Leibler Regularizer	634
20.12	Appendix: Multisource VSP and $[\mathbf{L}^T \mathbf{L}]^{-1}$	637
20.13	Appendix: Conditional Covariance Matrix	638
20.14	Appendix: Bayes and Conditional Covariance Matrix	640
20.15	Appendix: Estimation of Statistical Parameters for VSP Data	643
20.15.1	Estimating $p(\mathbf{d})$ and $p(\mathbf{m})$	643
20.15.2	Estimating $p(\mathbf{d} \mathbf{m})$	644
21	Discriminant Analysis and Gaussian Mixture Model	647
21.1	Introduction	647
21.2	Generative and Discriminative Models	649
21.3	Linear and Gaussian Discriminant Analysis	650
21.3.1	Linear Discriminant Analysis	651

21.3.2	Gaussian Discriminant Analysis	653
21.4	Theory of the Gaussian Mixture Model	657
21.4.1	Responsibility Function $p(k \mathbf{x}^{(n)})$	659
21.4.2	Expectation-Maximization Method	660
21.4.3	1D Example of a Responsibility Function	661
21.4.4	Geophysical Inversion	663
21.4.5	Example of Generative and Discriminative Modeling	663
21.4.6	Fuzzy Clustering and GMM	665
21.5	Numerical Examples of GMM in Geoscience	665
21.5.1	Turbidite Identification from Seismic Data	665
21.5.2	Gravity and Magnetic Inversion with GMM Constraints	667
21.5.3	Joint Inversion with Updated GMM Penalty Terms	671
21.6	Summary	672
21.7	Exercises	674
21.8	Computational Labs	676
21.9	Appendix: Gradients of the GDA Log-likelihood Function	676
21.9.1	Solving for ϕ	677
21.9.2	Solving for $\boldsymbol{\mu}$	678
21.9.3	Solving for $\boldsymbol{\Sigma}$	679
21.9.4	Gradient of the GMM Log-likelihood Function	679
VI	Seismic Inversion and Machine Learning	681
22	Physics-Informed Machine Learning Inversion	683
22.1	Deterministic and Stochastic Inversion	683
22.2	Incomplete Training and Physics-Informed ML	685
22.2.1	Data Skeletonization and ML	685
22.3	Physics-Informed Machine Learning	686
22.3.1	Sequential ML+Physics Inversion	687
22.3.2	Simultaneous ML+Physics Inversion	687
22.4	Automatic Differentiation	687
22.5	Summary	687
23	Tomographic Deconvolution	689
23.1	Introduction	689
23.1.1	Previous Work	690
23.2	Theory of Tomographic Deconvolution	691
23.2.1	Migration Deconvolution versus Tomographic Deconvolution	692
23.2.2	Tomographic Deconvolution Workflow	692
23.2.3	CNN Architecture	693
23.3	Numerical Results	694
23.3.1	Reflections: Single Anomaly Models	694
23.3.2	Reflections: Multiple Anomaly Models	695
23.3.3	Models that Break the Deconvolution Filter	695

23.3.4	Refractions: Multiple Anomaly Models	699
23.3.5	Refractions: Fault Anomaly Models	699
23.4	Summary	700
24	Neural Network Least Squares Migration	703
24.1	Introduction	703
24.2	Theory of Neural Network Least Squares Migration	705
24.2.1	Least Squares Migration	705
24.2.2	Sparse Least Squares Migration	706
24.2.3	Neural Network Least Squares Migration	707
24.2.4	Multilayer Neural Network LSM	709
24.3	Numerical Results	709
24.3.1	Three-layer Velocity Model	710
24.3.2	SEG/EAGE Salt Model	712
24.3.3	North Sea Data	714
24.4	Discussion	718
24.5	Conclusions	721
24.6	Appendix: Migration Green's Function	721
24.7	Appendix: Soft Thresholding Function	722
24.8	Appendix: Neural Network Least Squares Migration	723
24.9	Appendix: Alignment of the Filters	724
25	Wave Equation Inversion and Neural Networks	729
25.1	Introduction	729
25.2	Theory for Wave Equation Inversion of Skeletonized Data	731
25.2.1	Feature Extraction	732
25.3	NML Theory	733
25.4	NML Inversion of Crosswell Data	735
25.4.1	Assessing the Optimal Dimension of the Latent Space	736
25.5	NML Inversion of Refraction Data	737
25.6	Summary	742
25.7	Exercises	743
25.8	Connective Function	744
25.8.1	Gradient	745
26	Automatic Differentiation	747
26.0.1	Automatic Differentiation Algorithm	747
26.1	Modeling, Automatic Differentiation and Inversion	753
26.1.1	Automatic Differentiation for the One-way Wave Equation	753
26.1.2	Automatic Differentiation and Waveform Inversion	754
26.2	Summary	756
26.3	Exercises	756
26.4	FD Solution to the Wave Equation	757

VII Background Appendices	763
27 Appendix: Geophysics Background	765
27.1 Seismic Data Recording and Processing	765
27.2 Diffraction Stack Migration	772
27.3 Surface Waves	776
27.3.1 Estimating Depth vs Frequency	777
27.4 Seismic Reflection Data as an LTI System: $s(t) = r(t) \star w(t)$	777
28 Probability Theory for Machine Learning	783
28.1 Random Variables, Sample Space, Events and Probability	783
28.1.1 Types of Events	784
28.1.2 Probability	785
28.1.3 Law of Total Probability	790
28.2 Bayes' Theorem	793
28.2.1 Bayes' Theorem and Cancer Example	793
28.2.2 Bayes Theorem for K Disjoint Events	794
28.2.3 Bayesian Terminology	794
28.3 Gaussian Probability Distribution	795
28.3.1 Central Limit Theorem	796
28.3.2 Multivariate Normal Distribution	796
28.4 Sampling a Probability Distribution	798
28.5 Maximum Likelihood Estimate and Neural Network Models	798
28.6 Summary	800
28.7 Exercises	800

Preface

This book presents the theory of machine learning (ML) algorithms and their applications to geoscience problems. More than half of the described algorithms fall under the class of neural network methods. Their description is at a level that can be understood by anyone with a modest background in linear algebra, calculus and probability. An elementary working knowledge of MATLAB is assumed and almost every chapter is accompanied by lab exercises to reinforce the ML principles. If you don't know MATLAB or Python, many of the labs use the CoLab, aka Colaboratory, notebook which is an easy-to-use product from Google that allows for the execution of Keras-based ML computer codes. It also provides for the free use of a cloud-based GPU processor¹ that can be used as soon as you login. There is no need for the troublesome installation of notebook software.

There are many definitions of *machine learning* (ML), but one of the best is attributed to Arthur Samuel²:

Machine learning is the field of study that gives computers the ability to learn without being explicitly programmed.

This definition doesn't mean we don't have to write the programs, it means that the ML algorithm finds the best model by learning from the data without relying on rules-based programming. For example, finding the best fit model $\mathbf{y} = f(\mathbf{x})$ by a typical least squares procedure typically assumes a linear mathematical model $f(\mathbf{x})$ that predicts the output \mathbf{y} from the input \mathbf{x} . For example, $\mathbf{W}\mathbf{x} = \mathbf{y}$, where \mathbf{W} is a matrix. A ML algorithm such as a neural network avoids this assumption by devising the best non-linear model learned from the data \mathbf{y} for the given architecture.

Neural Network Example. How does the neural network learn the model³ $f(\mathbf{x}) = \mathbf{y}$ from the data? Learning the model $f(\mathbf{x})$ is accomplished by using a large training set of data $(\mathbf{x}^{(n)}, \mathbf{y}^{(n)})$ for $n \in \{1, 2, \dots, N\}$, and adjusting the parameters of the model until $f(\mathbf{x}^{(n)})$ can accurately predict $\mathbf{y}^{(n)}$ for any training pair. Once the model is learned, then it can accurately predict the output $f(\mathbf{x}^{new}) = \mathbf{y}^{new}$ from a new input \mathbf{x}^{new} . This can be important

¹Colab is a hosted Jupyter notebook service that requires no setup to use, while giving free access to computing resources including GPUs. See <https://colab.research.google.com/notebooks/intro.ipynb>

²This quote is often attributed to Arthur Samuel, but it cannot be found in Samuel (1959, 1967). A similar quote can be found at <https://www.techemergence.com/what-is-machine-learning/>. See <http://infolab.stanford.edu/pub/voy/museum/samuel.html> for a brief bio of this pioneering engineer.

³"Learning the model" is equivalent to computing the parameters of the non-linear function $f(\mathbf{x})$ that allow for an accurate prediction of $f(\mathbf{x}) = \mathbf{y}^{true}$ for all the training pairs $(\mathbf{x}, \mathbf{y}^{true})$.

for many applications, such as predicting the presence of underground contaminants \mathbf{y}^{new} from processed geoelectrical and/or seismic data \mathbf{x}^{new} , accurately detecting the presence of breast cancer \mathbf{y}^{new} recorded on a fusion of CAT scan and MRI images \mathbf{x}^{new} , or delineating the faults in \mathbf{y}^{new} on the right-hand side of Figure 1 from the input seismic section \mathbf{x}^{new} on the left-hand side.

The mathematical operations of a convolutional neural network model are represented by the block diagrams in Figure 1, where the input image \mathbf{x} of a seismic section is decomposed into component images contained in the FM1 block (or shallowest layer). Here, a block represents a set of mathematical operations that produce a stack of 2D images known as feature maps (FMs). Each of the 32 feature maps in FM1 is computed by convolving a small filter (3×3 filter in this example) with the input image, and then each pixel value in the FM is thresholded to be between 0 and 1 by a non-linear squashing function⁴. The FM1 feature maps are then subsampled by a factor of four (aka known as maxpooling), and the resulting images are filtered and thresholded by the FM2 3×3 filters to get the 64 FMs for block 2. The subsampling acts as a low-pass spatial filter so that only coarser features of the seismic section are seen in, for example, FM3. In the end, the FMs represent the decomposition of a complicated object into high-wavenumber images on the left and low-wavenumber images on the far right. The FMs are weighted, upsampled, summed together and squashed to make a single decision, i.e. classification, at each pixel associated with the input image (Long et al., 2015). Does the pixel value represent a fault, then the answer is yes $y = 1$ for its class. If not, then the answer is no $y = 0$ for the output class. The displayed FMs are upsampled by a deconvnet procedure to transform them to the same size as the input image.

Neural Networks and Deeper Connections. Neural network models lack a rigorous theoretical foundation that explains their formidable number of commercial successes. This has motivated physicists and mathematicians to search for its mathematical and physical foundations. For example, they have recently discovered that successful CNN modeling can have many more tunable parameters than training data, i.e. equations of constraint, without suffering from overfitting. Arora et al. (2018) proves that a large number of FMs can be redundant and allows for simple compression of the model.

Another insight says that the CNN decomposition is similar to a dictionary-learning algorithm (Papayan et al., 2016, 2017a, 2017b; Sulam et al., 2018), where the different FMs can represent the multiscale components of a complicated object, such as its atoms or molecules. As an example, Figure 2 illustrates how two convolutional FMs, denoted as elementary "atoms" in the bottom row, are combined and filtered to create slightly more complex structures, i.e. molecules, at the second level. These "molecules" are then combined by a CNN model to create the global atom representing, in this case, a digit.

However, the basic operations of the neuron, i.e. atom, has much more complexity than previously thought, where the atom itself is composed of even finer structures. Work by Beniaguev et al. (2021) suggests that the cortical neuron mathematically performs the

⁴A squashing function $\sigma(z)$ *squashes* a wide range of input values $-\infty < z < \infty$ to be between a small range of output values such as $0 \leq \sigma(z) \leq 1$. The squashing operation sparsifies essential+extraneous information into its essential components (Papayan et al., 2016, 2017a, 2017b; Sulam et al., 2018; Chen et al., 2020b).

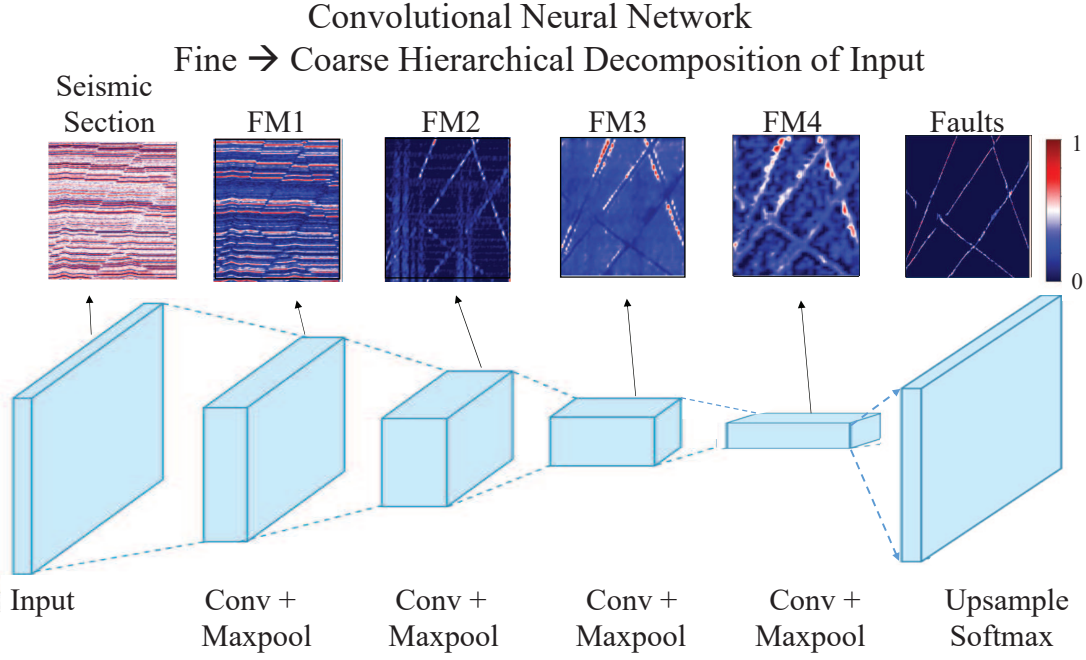


Figure 1: Block diagram of the convolutional neural network (CNN) architecture that decomposes the input picture of a seismic section into fine-scale feature maps (FM1 and FM2) and coarser-scale feature maps (FM3 and FM4). To provide a more interpretable image, the FMs are *deconvolved* for the display of interpretable images (Shi et al., 2018). The pixels in the far-right image are labeled $0 < y < 1$, where $y = 1$ indicates that the pixel is a fault and $0 \leq y \leq 1$ indicate the probability of being a fault. Typically, the shallow 3×3 filters that compute the 32 FM1 images from the input image detect the sharp edges in the input, and the filters associated with FM2 to FM3 detect larger scale features such as the general shape of the fault. These *successive decompositions derive the building blocks at successive levels from specific combinations of building blocks at the previous level* (Holland, 1995). Figure partially adapted from Dertat (2017) and Shi et al. (2018).

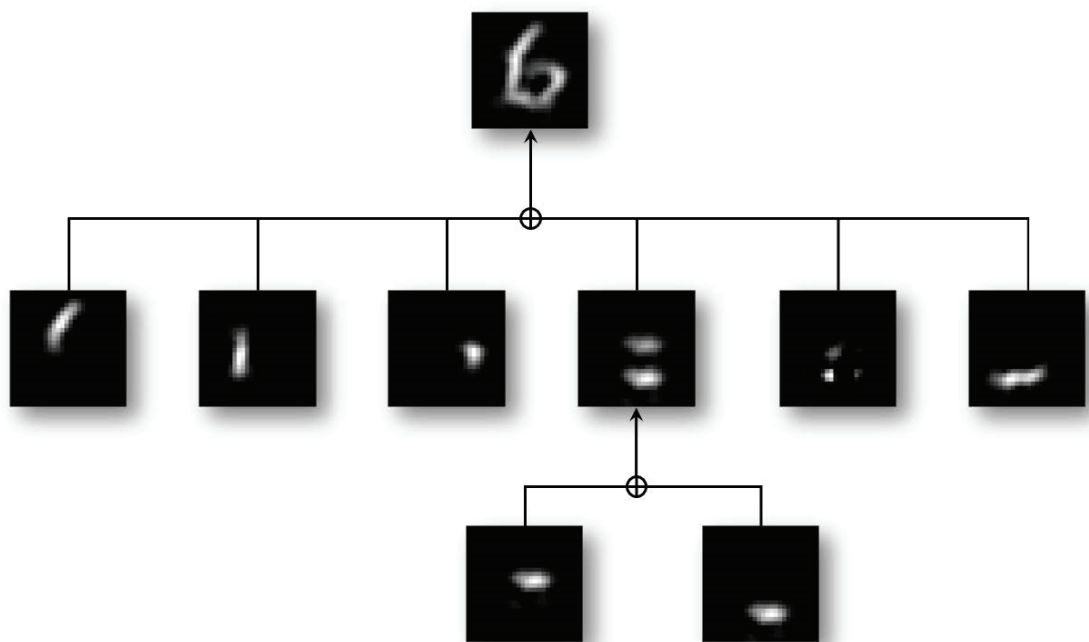


Figure 2: Elementary FMs in the bottom row are combined to form the molecules in the second row, which in turn are used to form the digit 6 in the top row. Figure from Sulam et al. (2018).

same functions as a deep neural network with 5-8 layers. This depth is associated with the neuron’s dendritic branches that act as spatial pattern detectors.

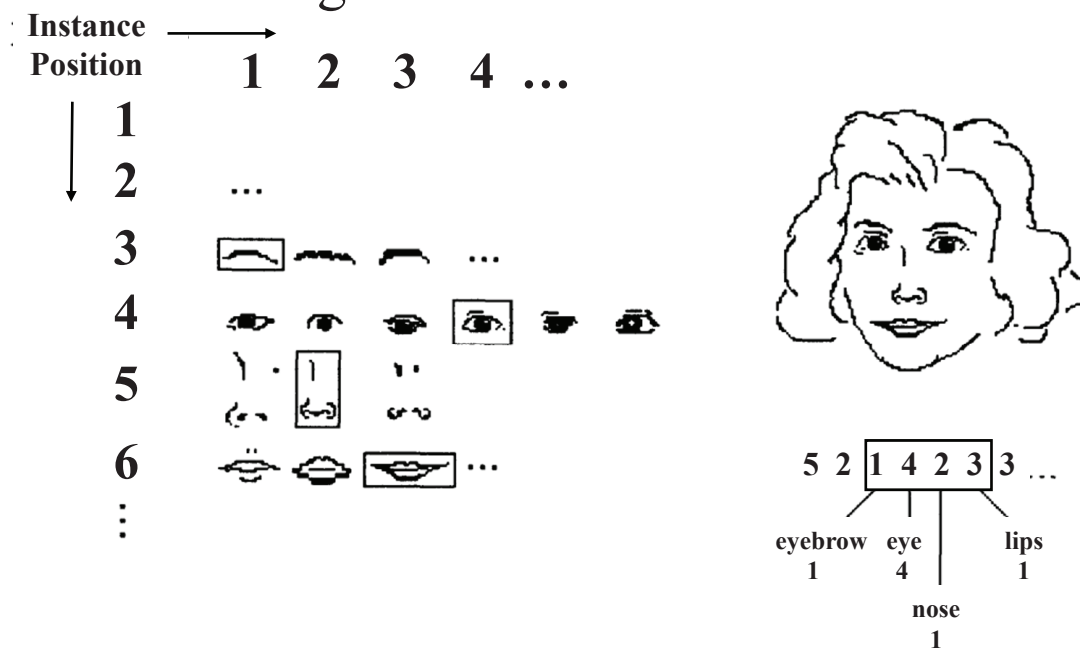
Decomposing an input image into a sequence of simpler-to-more complicated parts is also used to describe the process of adaptive evolution illustrated in Figure 3. John Holland (1995) describes the fundamental set of procedures for adaptive evolution in nature:

‘If model making, broadly interpreted, encompasses most of scientific activity, then the search for building blocks becomes the technique for advancing that activity. At a fundamental level, we have the quarks of Gell-Mann. Quarks can be combined to yield nucleons, the building blocks at the next level. The process can be iterated, deriving the building blocks at successive levels from specific combinations of building blocks at the previous level. The result is the quark/ nucleon/ atom/ molecule/ organelle/cell/ underpins much of physical science.’

Artificial Intelligence and CNN. More generally, ML methods belong to the larger class of artificial intelligence⁵ algorithms (see Figure 4), but the one that is attracting the most interest is that of deep learning with CNNs. Convolutional neural networks are now playing leading roles in the software for self-driving cars, language translation, speech recognition, computer vision, fusion and diagnosis of medical images, analysis of satellite and aerial

⁵<https://blogs.nvidia.com/blog/2016/07/29/whats-difference-artificial-intelligence-machine-learning-deep-learning-ai/>

Building Blocks and Recombination



A face can be described by stringing together the numbers that index its different component parts.

Figure 3: Neural networks is similar to John Holland's (1995) description of how nature evolves models: '...building blocks at successive levels from specific combinations of building blocks at the previous level.'. The important features of the face are denoted by the *feature* rectangles on the left. Figure adapted from Holland (1995).

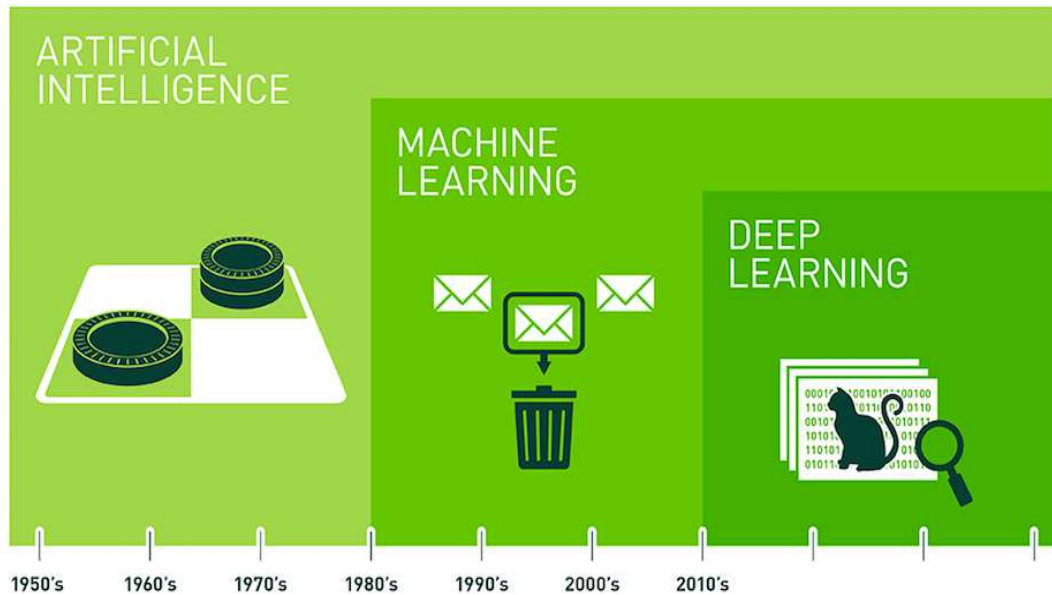


Figure 4: Artificial intelligence (AI) and the sub-classes of machine learning and deep learning, where AI involves a machine doing something that only a human would be able to do. Source of picture is Nvidia.

images for optimizing agricultural practices, and many other fields. Significantly, it is now being recognized as an important interpretation tool for analyzing lithology from seismic and well-log data, detecting faults in large 3D volumes of seismic data, and searching for patterns in earthquake data.

Organization of the Book. This book is divided into six main sections:

- **Mathematical Background and Optimization Theory.** Optimization theory and gradient descent methods for ML are reviewed, with an emphasis on the choice of step length methods. Readers with a familiarity of these algorithms can skip to the next sections.
- **Supervised Learning Algorithms.** Introduction to neural networks, fully-connected neural networks, applications to geoscience problems, and support vector machines.
- **Convolutional Neural Networks.** Basics of convolution and correlation, CNN, object identification, semantic segmentation, recurrent neural networks, Transformers and self-attention.
- **Unsupervised Learning Algorithms:** Autoencoders, convolutional sparse coding, principal component analysis, clustering methods, generative adversarial networks.
- **Bayesian Analysis.** Sampling, Bayes' theorem, and Gaussian mixture models.

- Seismic Inversion and ML. Physics-informed ML inversion, tomographic deconvolution, neural network LSM, wave equation inversion and neural networks, automatic differentiation.

Most chapters are accompanied by executable code (MATLAB and/or Keras with CoLab) that can be implemented by the reader with a modest level of programming knowledge. The understanding of the algorithms is deepened by parameter tuning and by examining the details of the code. Most of these codes have been written by my co-authors, without which this book would not have been written.

Case histories are used to demonstrate the practical use of ML in solving geoscience problems. These problems include fracture identification in photos, detection of rock cracks in drone photos, fossil and lithology detection in thin sections, prediction of permeability in rock samples, geochemical analysis, well-log analysis and identification of salt boundaries in seismic data, seismic arrival-time picking by a clustering method, least squares migration, velocity analysis, demultiple, noise reduction in seismic data and migration images, and some interpretation examples for seismic and radar data. The reader who diligently goes through the chapters and labs will have a thorough grounding in some of the fundamental ML methods used in geoscience.

WWW Software Sites for Computational Labs. The computational labs for the book *Machine Learning in Geoscience* are located at the following sites:

- *Machine Learning in Geoscience* Labs: <http://csim.kaust.edu.sa/files/ErSE394/LAB1/>
- *Machine Learning in Geoscience* Labs: <http://utam.gg.utah.edu/books/ML/index.html>
- *Machine Learning in Geoscience* Labs: <http://seg.org/books/Schuster.ML/index.html>
- *Machine Learning in Geoscience* Labs: repository.kaust.edu.sa/bitstream/handle/10754/674007/GeoscienceMachineLearning.html
- *Machine Learning in Geoscience* Labs: <https://earth.utah.edu/books/Schuster.ML/index.html>

The computational labs for the books *Seismic Interferometry* and *Seismic Inversion* are located at the following sites:

- *Seismic Interferometry* Labs: <http://utam.gg.utah.edu/Inter.LAB1/>
- *Seismic Inversion* Labs: repository.kaust.edu.sa/bitstream/handle/10754/674016/SeismicInversion.html
- *Seismic Inversion* Labs: <https://earth.utah.edu/books/Schuster.SeismicInversion/index.html>

Acknowledgments

GTS is very thankful for the financial and computer support provided by King Abdullah University of Science and Technology and the KSL facilities (<https://www.hpc.kaust.edu.sa>)

/). The assistance of Professor Xiangliang Zhang (KAUST and Notre Dame University), Dr. David Pugh (KSL) and Dr. Saber Feki (KSL) were very beneficial in bringing me to the frontiers of teaching ML. My loyal co-authors are to be acknowledged for writing many of the computer codes that accompany the chapters. I am very grateful to Professor Daniel Trad at Calgary University for his tireless editing of the manuscript. He provided many detailed comments and suggestions for improvement. I am deeply grateful to Dr. Yan Yang for discussions about modifications and her expert help in organizing and implementing corrections, and appreciate the faithful editing of the manuscript by my co-authors. This book benefitted from the inclusion of appendix 17.6.2 written by Yunsong Huang, the excellent geoscience examples provided by Eduardo Cano, Ahmad Ramdani and Tian Qiao, the concise summaries of many ML classes provided by Yuan Yang, and thorough lab instructions by Shi Yongxiang.